



## Kinetics, equilibrium and thermodynamics of ciprofloxacin hydrochloride removal by adsorption on coal fly ash and activated alumina

Monika Maheshwari\*, Raj K. Vyas, Manisha Sharma

*Department of Chemical Engineering, Malaviya National Institute of Technology, Jaipur 302017, India  
Tel. +91 9462865195; email: maheshwari.monika16@gmail.com*

Received 19 September 2012; Accepted 30 January 2013

---

### ABSTRACT

In this study, performance of two different adsorbents namely, activated alumina (AA) and coal fly ash (CFA) have been examined for the removal of an antibiotic Ciprofloxacin hydrochloride (CPH) from its aqueous solution. Batch adsorption experiments were conducted to study the effect of various operational parameters such as pH, initial antibiotic concentration, adsorbent dose, and temperature on the adsorption process. The optimal pH for CPH adsorption was found to be 4. The adsorption kinetics was evaluated at different initial antibiotic concentrations and temperatures. Kinetics of adsorption, in all cases, followed pseudo-second-order rate equation for both the adsorbents. Adsorption of CPH was well described by Freundlich isotherm. Thermodynamic analysis unveiled the feasibility, spontaneity, and endothermic nature of overall adsorption process at higher temperatures. Values of  $\Delta G^\circ$  for CFA and AA are  $-0.029$  and  $-2.714$  kJ/mol, respectively, at 328 K. The corresponding values for  $\Delta H^\circ$  are 6.572 and 28.408 kJ/mol and that of  $\Delta S^\circ$  are 0.020 and 0.093 kJ/mol K, respectively. The study is significant in designing the water treatment plants for the removal of CPH. Overall, it was concluded that AA is a better adsorbent than CFA for the removal of CPH from its aqueous solution.

*Keywords:* Ciprofloxacin hydrochloride; Coal fly ash; Activated alumina; Adsorption

---

### 1. Introduction

Pharmaceutical products like antibiotics, hormonal drugs, nutrition promoters, antiseptics, and anesthetics are widely being used for human treatment and veterinary purposes [1]. The surface water contaminated by wastewater effluents from municipal wastewater treatment plants is found to contain such pharmaceuticals. The major sources of antibiotic discharge are pharmaceutical industries, household waste, and hospitals.

Presence of antibiotics in water has its ecotoxicological effects on receiving water bodies [2]. Moreover, persistent low concentration of antibiotics may develop resistant bacterial strains in water bodies. Such strains have been reported in hospital effluents [3]. Therefore, it is desirable to remove such antibiotics from the effluent before their discharge into aqueous streams.

Ciprofloxacin hydrochloride (CPH) is a broad-spectrum antibiotic of fluoroquinolone group used to treat bacteria, rickettsia, and protozoa [4]. It is among the most widely prescribed antibiotics in the USA [5]

---

\*Corresponding author.

and is applicable on a variety of infectious processes such as gonococcal infections, osteomyelitis, enteric, respiratory, urinary tract infections [6], and deadly diseases like anthrax [4]. In hospital effluents, the concentration of CPH was reported to lie within the range of 0.7–124.5  $\mu\text{g/L}$  [7]. Brown et al. [8] reported the concentration of Ciprofloxacin of up to 2000 ng/L in hospital wastewater and 200–1,000 ng/L in influent of wastewater treatment plant. These concentrations of antibiotics reported in water bodies are a result of dilution of several times. Removal of CPH from water bodies at such a low concentration is a gigantic task. As such, it is desirable to remove CPH from the effluent before its discharge into the water bodies. In addition, CPH is not readily biodegradable in water [7]. The treatment of wastewater containing such antibiotics is extremely difficult, expensive, and creates problem to biological treatment processes [9]. Many processes for the treatment of fluoroquinolone containing water/wastewater are available. Methods, such as adsorption [10,11], electrochemical removal [3], photo-Fenton process [12], photocatalysis [13], ozonation and peroxone process [14], oxidation by chlorination [15], etc. have been investigated.

Adsorption, since past few years, has been an efficient method for removal of antibiotics from their aqueous solutions. The technique produces high-quality treated effluent and allows kinetic and equilibrium measurements without involving any highly sophisticated instruments. Coal fly ash (CFA), a low-cost adsorbent, is produced largely as a waste by-product of thermal power plant. India has been rated as the fourth largest producer of coal ash (as a by-product) in the world [16]. In addition, activated alumina (AA) has also been proved to be a good adsorbent for elements like boron, arsenic, selenium, vanadium anions, and fluoride [17–19]. AA and CFA are also widely in practice for adsorption of pollutants from water and wastewater. However, the experimental data on equilibrium and kinetic studies for the removal of CPH using these adsorbents are scarcely available. Previously adsorption of Ciprofloxacin on montmorillonite [20], hexagonal mesoporous silicate [21], activated carbon [22], modified CFA [23], goethite I [11], kaolinite [24], soil [25], etc. have been reported.

In this study, the removal of CPH using two different adsorbents CFA and AA has been studied. To the best of our knowledge, the adsorption of CPH on AA has not been reported so far. In India, near Patancheru, Hyderabad, a pharmaceutical effluent contained Ciprofloxacin as the most abundant drug with a concentration of about 31 mg/L [26]. Therefore, the CPH concentration range of

30–90 mg/L has been used in present study. Adsorption kinetics was examined at different initial concentrations and temperatures. Kinetic constants have been evaluated for pseudo-first-order, pseudo-second-order, Elovich, and intraparticle diffusion models. Equilibrium studies have also been analyzed using Langmuir, Freundlich, and Temkin isotherm models. The study can further be extended for the design of treatment plants especially in the pharmaceutical sector.

## 2. Experimental

### 2.1. Materials

CPH (Fig. 1) in pure form (M.W. = 385.82, Minimum assay: 98.0%, Melting Point: 318–320°C, Make: CDH, India) was used in the study.

Nitric acid (Minimum assay 72%/AR Grade) and ferric nitrate (M.W. 404, minimum assay: 98%, AR grade, Make: CDH, India) were used as reagents. The adsorbents, CFA was procured from Shree Power Cement, Beawer, Rajasthan, India and aluminum oxide active neutral (AA) (Mol. wt: 101.96) was obtained from Merck, India. The BET surface area of AA and CFA was found to be 105.31 and 3.701  $\text{m}^2/\text{g}$ , respectively. The adsorbents were used as such without any modification. Some additional properties of CFA and AA have been reported in Table 1.

### 2.2. Quantitative determination of CPH

The quantitative determination of CPH was conducted by measuring optical density at 435 nm on a UV-Visible spectrophotometer, (make: ECIL, Hyderabad, model: GS5075). A 100 mg/L stock solution of CPH was prepared by dissolving 100 mg of pure CPH in 1L of distilled water using a magnetic stirrer. Standard solutions within a concentration range of 20–100 mg/L of CPH were prepared from the stock solution. The coloring reagent (1% iron (III) nitrate solution (w/v) in 1% nitric acid (v/v)) was then added and the calibration curve ( $R^2=0.997$ ) was obtained [27].

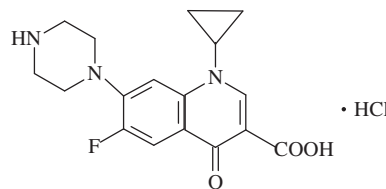


Fig. 1. Chemical structure of CPH.

Table 1  
CFA and AA characteristics

CFA		AA	
Particulars	Values <sup>a</sup>	Particulars	Values <sup>b</sup>
% Total moisture	0.92	Solubility	(20 °C) insoluble
% Solid matter	0.60	Melting point	2,050 °C
% Inert matter	0.32	Molar mass	101.96 g/mol
% Volatile matter	0.55	Density	3.94 g/cm <sup>3</sup> (20 °C)
% Ash	29.73	Bulk density	370–900 kg/m <sup>3</sup>
% Fixed carbon	61.40	pH value	5–8 (100 g/L, H <sub>2</sub> O, 20 °C) suspension
Net calorific value (kcal/kg)	5,780	Boiling point	2,980 °C
% Total carbon	14.40	Vapor pressure	(20 °C)

<sup>a</sup>As reported by Shree Cement, Beawer, Rajasthan, India.

<sup>b</sup>As reported by Merck Pvt Ltd.

### 2.3. Characterization

#### 2.3.1. Characterization of water sample containing CPH

In the present study, the concentration of CPH in water was correlated with wastewater parameters such as COD, electrical conductivity, pH, etc. Synthetic aqueous solution of CPH was prepared in distilled water. To prevent degradation, CPH solution was kept below 4 °C. COD, pH, and electrical conductivity of 30 mg/L CPH solution were experimentally determined as 84 mg/L, 5.5 and 238 μS, respectively.

#### 2.3.2. Scanning electron microscopy analysis of adsorbents

Surface and particle analysis by scanning electron microscope (make: JEOL Ltd., model: JSM 6610 LV) was conducted at 20 kV and 750X for AA and at 20 kV and 500X for CFA. The typical SEM images of both the adsorbents have been shown in Fig. 2(a) and (b). It may be observed from the figure that the adsorbent surfaces have irregular or round form with surface defects. When carefully examined, particle diameters were found to range from tens to hundreds of micrometers.

### 2.4. Adsorption process

Batch studies were performed to examine the influence of temperature, pH, initial antibiotic concentration, and adsorbent dose on the uptake rate of CPH. A fixed volume of CPH solution (30 mg/L) and requisite quantity of AA were taken in a conical flask. The flask was then agitated and aliquots were taken at a fixed time interval and filtered using Whatmann filter paper No. 42 followed by spectrophotometric measurement. Similar experiments were also conducted using CFA.

### 2.5. Adsorption kinetics

The adsorption process requires knowledge of diffusion mass transport or kinetic process for different adsorbents. Therefore, models such as pseudo-first-order [28], pseudo-second-order [29], intraparticle diffusion [28], and Elovich kinetic model [30–32] were employed to analyze the adsorption kinetic data.

#### 2.5.1. Pseudo-first-order kinetic model

The linearized pseudo-first-order kinetic equation is expressed as:

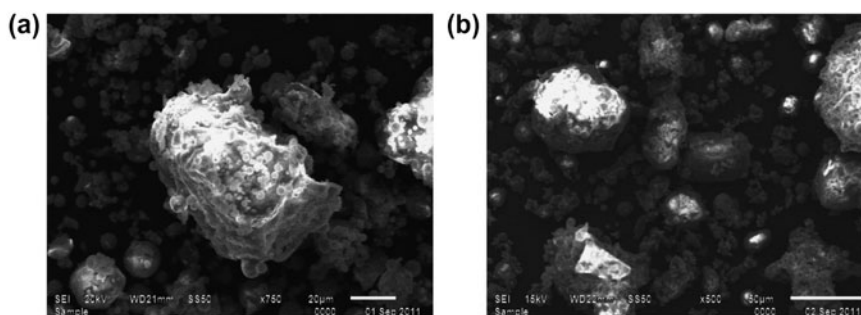


Fig. 2. (a) SEM images of (a) AA at 20 kV and 750X and (b) CFA at 20 kV and 500X.

$$\log(q_e - q_t) = \log(q_e) - \frac{k_1}{2.303}t \quad (1)$$

If the pseudo-first-order kinetics is applicable, a plot of  $\log(q_e - q_t)$  vs.  $t$  should provide a linear relationship. The constants  $k_1$  and predicted  $q_e$ , respectively, can be determined from the slope and intercept of the plot.

### 2.5.2. Pseudo-second-order kinetic model

Integrated rate equation for pseudo-second-order model is given as:

$$\frac{t}{q_t} = \frac{1}{k_2 q_e^2} \frac{1}{q_e} t \quad (2)$$

Values of  $k_2$  and  $q_e$  can be calculated from the corresponding intercept and slope of the linear plot of  $t/q_t$  vs.  $t$ . A linear relationship obtained from the plot indicates that the pseudo-second-order kinetics is applicable.

The initial sorption rate ( $h$ ) may be calculated by the following expression [32]:

$$h = k_2 q_e^2 \quad (3)$$

### 2.5.3. Elovich kinetic model

Elovich kinetic equation is another rate equation based on adsorption capacity, which is generally expressed as:

$$\frac{dq_t}{dt} = \alpha e^{-\beta q_t} \quad (4)$$

Integrating Eq. (4), assuming  $\alpha\beta t \gg 1$  for simplification and by applying boundary conditions  $q_t=0$  at  $t=0$  and  $q_t=q_t$  and  $t=t$ , we get:

$$q_t = \frac{1}{\beta} \ln(\alpha\beta) + \frac{1}{\beta} \ln(t) \quad (5)$$

A linear relationship is obtained on plotting  $q_t$  vs.  $\ln t$  with a slope of  $(1/\beta)$  and an intercept of  $(1/\beta) \times \ln(\alpha\beta)$ , in case CPH adsorption fits the Elovich model. The constants of the model can be obtained from the slope and intercept.

### 2.5.4. Intraparticle diffusion model

The adsorption process is a multistep process involving the transport of solute molecules from the aqueous phase to the surface of the solid particles followed by diffusion of the solute molecules into the

interior of the pores. The second-step diffusion is usually a slow process, and is therefore, rate-determining step. The intraparticle diffusion model is represented using the following equation [28,31,33]:

$$q_t = K_{\text{dif}} t^{0.5} + C^* \quad (6)$$

The plot of  $q_t$  vs.  $t^{0.5}$  may present a multilinearity correlation indicating that two or more steps occur during adsorption process. The intraparticle rate constant  $K_{\text{dif}}$  is directly evaluated from the slope of the regression line and  $C^*$  by the intercept. The values of  $C^*$  provide information about the thickness of the boundary layer.

### 2.6. Adsorption isotherms

Adsorption equilibrium studies describe the relation between the amount of adsorbate that accumulates on the adsorbent and the equilibrium concentration of the dissolved adsorbate. To determine the adsorption isotherm, experiments were performed with 100 mL CPH solution (20–80 mg/L) and 0.1 g of precisely weighed amount of adsorbent (1 g/L). The flasks were agitated at 25°C in a controlled shaker at about 200 rpm till equilibrium. These samples were then filtered prior to spectrophotometric analysis. Present investigation is concerned with the major isotherm models, namely Langmuir, Freundlich, and Temkin isotherms for both the adsorbents. After determining the  $q_e$  value, the isotherms were plotted.

#### 2.6.1. Langmuir isotherm

The Langmuir isotherm assumes that sorption is localized in a monolayer and no interaction between the adsorbate molecules exists. Moreover, the adsorbent surface is homogeneous so, adsorption energy is constant over all sites. The Langmuir isotherm model is expressed as [34]:

$$q_e = \frac{q_m b C_e}{1 + b C_e} \quad (7)$$

Linearized form of Langmuir equation may be presented as:

$$\frac{1}{q_e} = \frac{1}{q_m} + \frac{1}{K_L q_m C_e} \quad (8)$$

Langmuir constant ( $K_L$ ) is related to the maximum adsorption capacity (Langmuir monolayer adsorption capacity) and the energy of adsorption, respectively. These constants can be evaluated from the intercept

and the slope of the linear plot of experimental data of  $1/q_e$  vs.  $1/C_e$ .

The essential characteristics of the Langmuir isotherm can be expressed by separation or equilibrium parameter, a dimensionless constant as:

$$R_L = 1/(1 + K_L C_0) \quad (9)$$

$R_L$  indicates the nature of the adsorption process as follows:

- $R_L > 1$ , Unfavorable,
- $R_L = 1$ , Linear,
- $0 < R_L < 1$ , Favorable,
- $R_L = 0$ , Irreversible.

The values of  $R_L$  in the range of 0–1 indicate that the adsorption process is favorable for both adsorbents. In addition, the Freundlich adsorption constant,  $n$ , should be within 1–10 for significant adsorption.

### 2.6.2. Freundlich isotherm

The Freundlich isotherm assumes the heterogeneity of the surface and that the adsorption occurs at sites with different energy of adsorption. The energy of adsorption is a function of the surface coverage. Eq. (10) represents the Freundlich isotherm [35]

$$q_e = K_f C_e^{1/n_F} \quad (10)$$

where  $K_f$  is the Freundlich constant and  $n_F$  the heterogeneity factor.

The value of  $K_f$  is related to the adsorption capacity of the adsorbent and value of  $1/n_F$  is related to the adsorption intensity. Following equation shows Freundlich isotherm in linear form:

$$\log q_e = \log k_f + \frac{1}{n_F} \log C_e \quad (11)$$

### 2.6.3. Temkin isotherm

The Temkin isotherm model assumes effect of some indirect interactions among adsorbate particles and suggests a linear decrease in the heat of adsorption of all the molecules in the layer [36].

Expression for Temkin isotherm is given as

$$q_e = B \ln a_T + B \ln C_e \quad (12)$$

where

$$B = \frac{RT}{b_T}$$

By plotting  $q_e$  against  $\ln C_e$ , the Temkin constants  $a_T$  and  $b_T$  can be obtained from intercept and slope, respectively.

### 2.7. Error analysis

To evaluate and compare the performance of kinetics and isotherm models, average relative error (ARE) and root-mean-square error (RMSE) were also evaluated [37].

ARE% is defined as:

$$\text{ARE}\% = \frac{100}{n} \sum_{i=1}^n \left| \frac{q_{\text{exp}} - q_{\text{calc}}}{q_{\text{exp}}} \right|_i \quad (13)$$

This error function attempts to minimize the fractional error distribution over the entire range of concentration.

RMSE% is defined as:

$$\text{RMSE}\% = \sqrt{\frac{1}{n} \sum_{i=1}^n \left( \frac{q_{\text{exp}} - q_{\text{calc}}}{q_{\text{exp}}} \times 100 \right)_i^2} \quad (14)$$

where  $q_{\text{calc}}$  is the predicted value at point  $i$ ,  $q_{\text{exp}}$  is the observed value at point  $i$ , and  $n$  is the number of data.

### 2.8. Thermodynamic study

Using adsorption data at different temperatures, various thermodynamic parameters of the adsorption systems such as change in Gibb's free energy ( $\Delta G^\circ$ ) were calculated as:

$$\Delta G^\circ = -RT \ln K \quad (15)$$

Enthalpy change ( $\Delta H^\circ$ ) and entropy change ( $\Delta S^\circ$ ) may be determined from Van't Hoff equation (18):

$$\ln K = \frac{\Delta S^\circ}{R} - \frac{\Delta H^\circ}{RT} \quad (16)$$

where  $K$  is ratio of  $q_e$  and  $C_e$ ,  $R$  is the universal gas constant (8.314 J/molK), and  $T$  is temperature in Kelvin. By plotting  $\ln K$  as ordinate and  $1/T$  as abscissa, values for  $\Delta S^\circ$  and  $\Delta H^\circ$  can be estimated. In present study, thermodynamic parameters were evaluated to ascertain the nature of adsorption.

## 3. Results and discussion

Constants of different kinetic models at different temperatures and initial CPH concentrations have

Table 2  
Kinetic study and error analysis of adsorption kinetics for the removal of CPH by AA and CFA at different initial CPH concentrations (temperature = 25°C and AA and CFA dose = 1 g/L, pH = 5.5)

Adsorbent	Initial CPH concentration mg/L	$q_{e,exp}$ (mg/g)	Pseudo-first order kinetics		Error analysis		Pseudo-second order kinetics		Error analysis				
			$q_{e,calc}$ (mg/g)	$k_1$ ( $\text{min}^{-1}$ )	$R^2$	ARE %	RMSE %	$q_{e,calc}$ (mg/g)	$k_2$ (g/mg min)	$h$ (mg/g min)	$R^2$	ARE %	RMSE %
CFA	30	13.41	10.56	0.0043	0.97	44.10	46.48	12.320	0.0011	0.16	0.99	6.72	8.71
	60	25.29	23.56	0.0091	0.88	28.07	31.21	28.868	0.0004	0.37	0.96	6.93	9.46
	90	54.04	40.2	0.0104	0.92	35.84	38.01	60.278	0.0003	1.21	0.97	8.24	11.59
AA	30	15.50	13.78	0.0085	0.90	19.03	22.06	19.845	0.0005	0.18	0.92	9.77	13.5
	60	33.62	32.17	0.011	0.88	10.61	17.45	38.066	0.0004	0.60	0.96	7.32	9.15
	90	58.62	46.19	0.0138	0.99	28.36	29.53	67.024	0.0003	1.60	0.99	1.02	1.19

Table 3  
Kinetic study and error analysis of adsorption kinetics for the removal of CPH by AA and CFA at different temperatures (AA and CFA dose = 1 g/L; contact time = 270 min, initial CPH concentration = 30 mg/L and pH = 5.5)

Adsorbent	Temperature (°C)	$q_{e,exp}$ (mg/g)	Pseudo-first order kinetics		Error analysis		Pseudo-second order kinetics		Error analysis				
			$q_{e,calc}$ (mg/g)	$k_1$ ( $\text{min}^{-1}$ )	$R^2$	ARE %	RMSE %	$q_{e,calc}$ (mg/g)	$k_2$ (g/mg min)	$h$ (mg/g min)	$R^2$	ARE %	RMSE %
CFA	25	13.41	10.67	0.0046	0.99	49.34	52.4	12.66	0.0010	0.162	0.99	11.74	13.67
	35	13.83	8.204	0.0046	0.90	63.57	64.75	13.16	0.0021	0.367	0.97	7.78	9.82
	45	14.87	11.87	0.0048	0.85	37.79	43.53	13.60	0.0011	0.199	0.91	15.05	18.89
	55	15.08	11.40	0.0023	0.97	59.23	60.76	13.89	0.0010	0.201	0.99	7.69	8.98
AA	25	14.25	7.69	0.0092	0.79	93.18	93.21	15.62	0.0018	0.449	0.98	7.64	1.01
	35	15.5	13.80	0.0087	0.90	18.92	21.97	19.86	0.0005	0.185	0.92	9.78	13.51
	45	17.37	19.04	0.0001	0.97	67.00	62.33	25.70	0.0003	0.186	0.97	35.35	34.47
	55	21.95	18.45	0.0046	0.70	87.72	81.63	21.27	0.0007	0.317	0.89	46.71	43.85

been estimated. Effect of various parameters like temperature, pH, initial CPH concentration, and adsorbent dose on the adsorption of CPH has been studied. Besides this, the equilibrium isotherm studies have also been conducted to evaluate the isotherm constants.

### 3.1. Kinetic studies

Four major types of kinetic models namely, pseudo-first-order, pseudo-second-order, Elovich, and intraparticle diffusion model were examined for the adsorption of CPH on AA and CFA at an initial CPH concentration (30, 60, and 90 mg/L) and temperature (25, 35, 45, and 55°C).

The corresponding values of kinetic rate constants and the corresponding linear regression correlation coefficient values for each parameter have been presented in Tables 2 and 3, respectively. From Tables 2 and 3, it is difficult to predict the best fitted kinetic model since the values of  $R^2$  for both pseudo-first-order kinetics and pseudo-second-order kinetics are in close agreement. In order to get the best fit, error analysis was conducted.

Tables 2 and 3 also show the error calculation results for both pseudo-first-order and pseudo-second-order kinetics at different initial concentrations of CPH and at different temperatures. From both Tables, low values of RMSE and ARE for pseudo-second-order kinetics confirm its applicability. It can, therefore, be concluded that the adsorption kinetics are well represented by pseudo-second-order kinetic model suggesting chemisorption behavior [38]. However, thermodynamics assay would be more appropriate to determine whether the process is governed by physisorption or chemisorption.

In pseudo-second-order model, the values of  $k_2$ ,  $q_{e,exp}$ ,  $q_{e,calc}$ , and  $h$  increased with increase in concentration and temperature. From Table 2, it can be seen that the values of initial sorption rate ( $h$ ) are higher

for AA compared to CFA. The values of  $h$  were found to increase with increase in CPH concentration which may be due to an increase in driving force at higher concentration.

In addition, Elovich model was also studied for the same set of data. Similar to pseudo-second-order kinetics, this model is based on the adsorption capacity. From Table 4, values of initial rate of adsorption ( $\alpha$ ) increase with increase in concentration of CPH. It shows that both adsorbents at high concentration exhibit a high adsorption capacity. Moreover, when the values of  $\alpha$  for both the adsorbents were compared, AA exhibited higher adsorption rate.

To investigate the controlling mechanism in adsorption kinetics, intraparticle diffusion model was also examined. Since the plot of  $q$  vs.  $t^{1/2}$  did not pass through origin, intraparticle diffusion cannot be considered as the sole rate-controlling step. The increase in the values of  $k_{dif}$  with increase in temperature indicates an increase in mobility of the CPH molecules. Moreover, increased values of  $C^*$  corresponds to a greater boundary layer diffusion effect.

Tables 4 and 5 show that initial adsorption rate is always better than desorption rate predicting high temperature is favorable for present adsorption process. The values of  $k_2$ ,  $q_{e,exp}$ ,  $q_{e,calc}$ , and  $h$  increased with increase in temperature. Again, in both cases of adsorbents, intraparticle diffusion cannot be considered as the sole rate-controlling step.

### 3.2. Adsorption isotherms

To determine the adsorption capacity of adsorbents, equilibrium study was performed to analyze the experimental data using well-known Langmuir, Freundlich, and Temkin models at 25°C and pH 5.5.

#### 3.2.1. Langmuir isotherm

Langmuir adsorption isotherm is a well-known isotherm model to explain the equilibrium data for many

Table 4

Kinetic parameters for adsorption of CPH at different initial CPH concentrations (temperature = 25°C and AA and CFA dose = 1 g/L, pH = 5.5)

Adsorbent	Initial CPH concentration (mg/L)	Elovich kinetic model			Intraparticle diffusion		
		$\alpha$ (mg/g min)	$\beta$ (g/mg)	$R^2$	$K_{dif}$ (mg/g min <sup>0.5</sup> )	$C^*$ (mg/g)	$R^2$
CFA	30	0.342	0.358	0.99	0.571	0.869	0.98
	60	0.852	0.161	0.94	1.304	2.299	0.98
	90	4.253	0.092	0.86	2.342	15.228	0.92
AA	30	0.422	0.229	0.91	0.882	0.497	0.88
	60	1.569	0.131	0.94	1.627	5.967	0.99
	90	3.644	0.070	0.99	2.898	15.292	0.94

Table 5

Kinetic parameters for adsorption of CPH at different temperatures (AA and CFA dose = 1 g/L; contact time = 270 min, initial CPH concentration = 30 mg/L and pH = 5.5)

Adsorbent	Temperature (°C)	Elovich kinetic model			Intraparticle diffusion		
		$\alpha$ (mg/g min)	$\beta$ (g/mg)	$R^2$	$K_{dif}$ (mg/g min <sup>0.5</sup> )	$C^*$ (mg/g)	$R^2$
CFA	25	0.335	0.349	0.99	0.588	0.746	0.99
	35	2.234	0.495	0.87	0.431	4.881	0.94
	45	0.476	0.349	0.87	0.602	1.598	0.91
	55	0.412	0.317	0.99	0.638	1.260	0.96
AA	25	0.916	0.286	0.85	0.748	3.577	0.76
	35	0.421	0.229	0.91	0.883	0.488	0.88
	45	0.401	0.174	0.98	1.182	1.434	0.97
	55	1.023	0.247	0.77	0.875	3.726	0.84

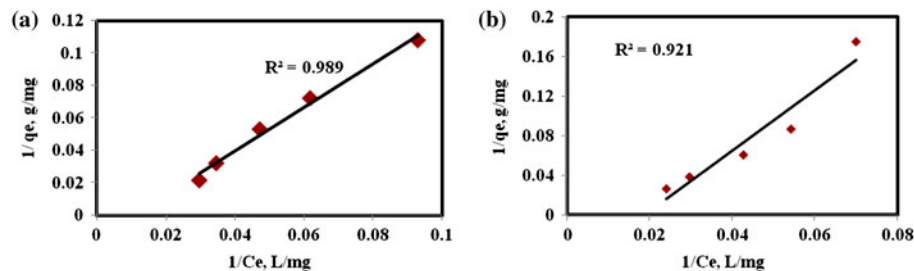


Fig. 3. Langmuir isotherm for adsorption of CPH on (a) AA and (b) CFA (AA and CFA dose = 1 g/L, pH 5.5, and temperature = 25°C).

adsorption processes. Langmuir isotherm plots and the corresponding Langmuir constants obtained from the plots for removal of CPH by AA and CFA have been presented in Fig. 3 and Table 6, respectively. Although, the Langmuir plot for AA exhibits a high linear

regression coefficient, the negative Langmuir constants indicate the non-applicability of this isotherm [39–42].

### 3.2.2. Freundlich isotherm

The linear plots in Fig. 4 illustrate that Freundlich isotherm is suitable for adsorption of CPH on both AA and CFA with  $R^2$  value of 0.969 and 0.975, respectively. The favorability of Freundlich isotherm indicates the heterogeneity. From Table 6, it may be observed that the slope of isotherm ( $1/n_f > 1$ ) implies cooperative adsorption [36]. The values of Freundlich isotherm constant  $K_f$ , clearly indicate higher adsorption capacity for AA (about four times) as compared to that of CFA. CFA with a variety of exchange sites on the ash surface has a CEC of about 25 mmol/100 g solid. On the other hand, CPH is known to possess a net positive charge in aqueous solution. Thus, there seems a possibility of ionic interactions which may contribute to the adsorption capacity of CFA. However, the adsorption properties of CFA can be improved further by adopting a suitable modification procedure. CFA with a higher adsorption capacity (1.55 mg/g) was obtained upon its modification [23] as compared to that of raw CFA used in the present study.

Table 6

Comparison of isotherm parameters for removal of CPH adsorption onto AA and CFA

Langmuir isotherm			
Adsorbent	$K_L$ (L/mg)	Max. Adsorption capacity ( $q_m$ ) (mg/g)	$R^2$
CFA	-0.019	-17.54	0.921
AA	-0.010	-71.43	0.989
Freundlich isotherm			
Adsorbent	$K_f$ (mg/g) ( $L/g$ ) <sup>n</sup>	1/n	$R^2$
CFA	0.078	1.665	0.975
AA	0.321	1.375	0.969
Temkin isotherm			
Adsorbent	B	$a_T$ (L/g)	$R^2$
CFA	28.78	0.081	0.963
AA	30.19	0.108	0.851

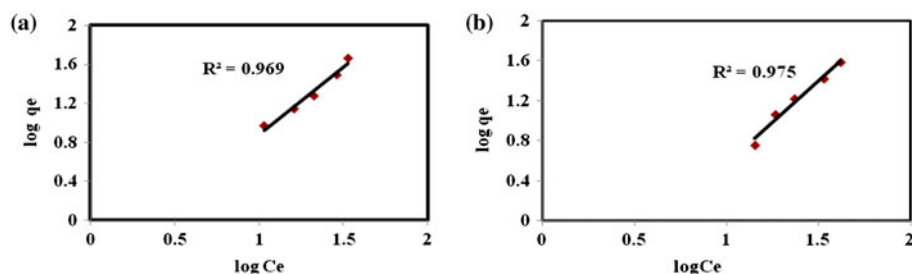


Fig. 4. Freundlich isotherm for adsorption of CPH on (a) AA and (b) CFA (AA and CFA dose=1g/L, pH 5.5, and temperature = 25°C).

### 3.2.3. Temkin isotherm

The sorption data were analyzed according to the linear form of Temkin isotherm (Fig. 5). It may be observed from the  $R^2$  values that Temkin isotherm complies with the experimental data for CFA while for AA, a low  $R^2$  value (0.851) implies the non-applicability of Temkin isotherm for the adsorption of CPH. However, as indicated by low values of  $b_T$  (0.082 kJ/mol for AA and 0.086 kJ/mol for CFA), sorbate–sorbent interactions in both cases of AA and CFA are neither purely by ion-exchange nor by physisorption.

### 3.3. Effect of temperature

Effect of temperature on adsorption of CPH from wastewater onto AA and CFA was investigated and the results have been shown in Fig. 6.

As observed from Fig. 6, the removal of CPH, in case of CFA, increased from 44.73% to 50.28% on increasing the temperature from 25 to 55°C. However, for AA, the corresponding percent removal of CPH significantly increased from 47.5% to 74%. This can be attributed to the fact that CPH removal from aqueous solution is facilitated at higher temperatures. The results, therefore, reflect the endothermic nature of adsorption suggesting the essentiality of the thermodynamic studies to ascertain the nature of the process.

### 3.4. Effect of pH

The effect of pH on the adsorption of CPH was studied at a pH range of 4, 7, and 10 (Fig. 7(a) and (b)). pH was found to significantly affect the removal of CPH. The maximum removal of 76.67% and 48.89% for AA and CFA, respectively was obtained at pH 4.

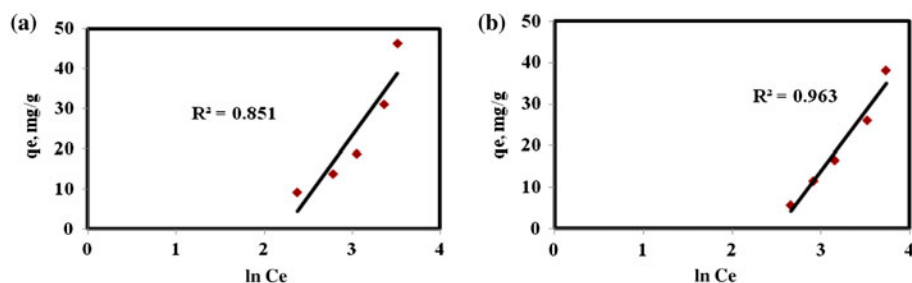


Fig. 5. Temkin isotherm for adsorption of CPH on (a) AA and (b) CFA (AA and CFA dosage=1g/L, pH 5.5, and temperature = 25°C).

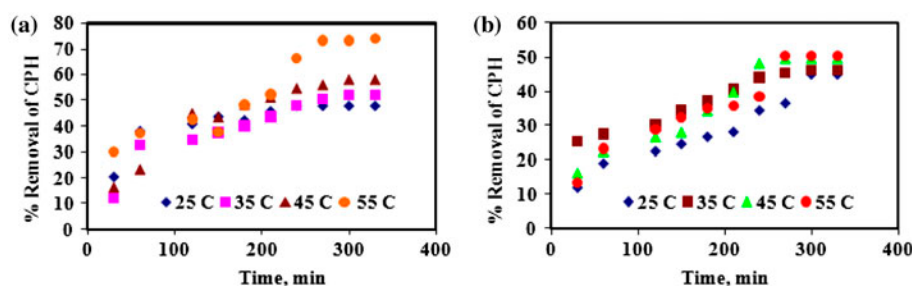


Fig. 6. Percent Removal of CPH at different temperatures for adsorption onto (a) AA and (b) CFA (AA and CFA dose = 1 g/L; Initial CPH concentration = 30 mg/L; and pH = 5.5).

Moreover, the percent removal of CPH was found to decrease with increase in pH. This behavior may be attributed to the zwitterionic properties of Ciprofloxacin. The pKa values of the CPH is approximately 6–8 [43]. In acidic medium (low pH), CPH is positively charged. The adsorbents, on the other hand, possess a net negative structural charge at low pH [44]. From Fig. 7, it is obvious that in acidic solutions, high ionic interactions occur between the cationic adsorbate and adsorbents' surface. Because of these interactions, high removal of CPH is accomplished. At pH 7, where the dominant solution phase species is the zwitterion, a cationic state can still be accepted as a major contributor to sorption since a

considerable amount of adsorbate was removed from the solution. However, at pH 10, the anionic state of CPH leads to a significant decrease in sorption capacity of adsorbents.

### 3.5. Effect of adsorbent dose

The effect of adsorbent dose on removal of CPH was investigated with adsorbent dose in the range of 0.1–20 g/L at 298 K, pH 4 with an initial CPH concentration of 30 mg/L (Fig. 8).

As evident from Fig. 8, the amount of CPH adsorbed increased from around 40% to 98% when AA dose was increased from 0.1 to 5 g/L because of

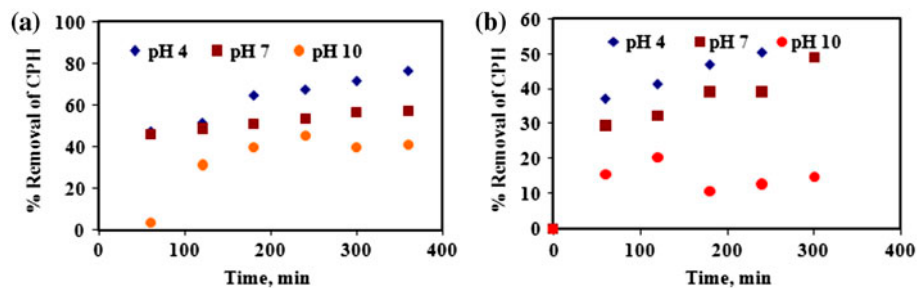


Fig. 7. Percent removal of CPH at different pH for (a) AA and (b) CFA (dose of adsorbents = 1 g/L; Initial CPH concentration = 30 mg/L; and temperature = 25°C).

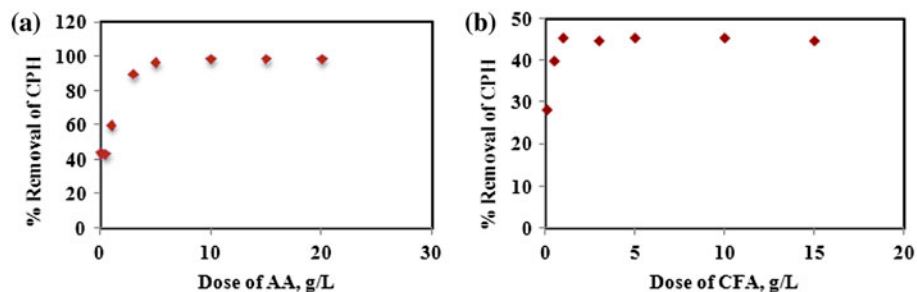


Fig. 8. Removal of CPH with different initial adsorbent doses of (a) AA and (b) CFA (initial CPH concentration = 30 mg/L, temperature = 25°C, pH 5.5).

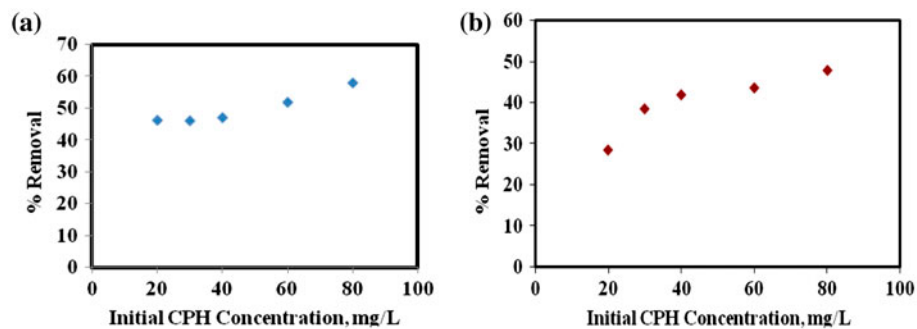


Fig. 9. Removal of CPH with different initial CPH concentrations onto (a) AA and (b) CFA (AA and CFA dose = 1 g/L, pH 5.5, and temperature = 25°C).

the availability of larger surface area and adsorption sites. At a dose of 5 g/L, maximum removal is obtained. For CFA, percent removal increased from around 28% to 46% up to dose of 1 g/L. After that, removal becomes constant. However, 60% removal was ascertained at 1 g/L of AA. Hence, AA in comparison to CFA, under similar operating conditions, exhibits higher adsorption.

### 3.6. Effect of Initial CPH concentration

The influence of initial CPH concentration on removal of CPH was investigated in the concentration range of 20–80 mg/L (Fig. 9).

It is evident from Fig. 9 that the removal increased with increase in initial CPH concentration. Percent removal, in case of AA, increased from 46.25% to 57.92% while for CFA it increased from 28.54% to

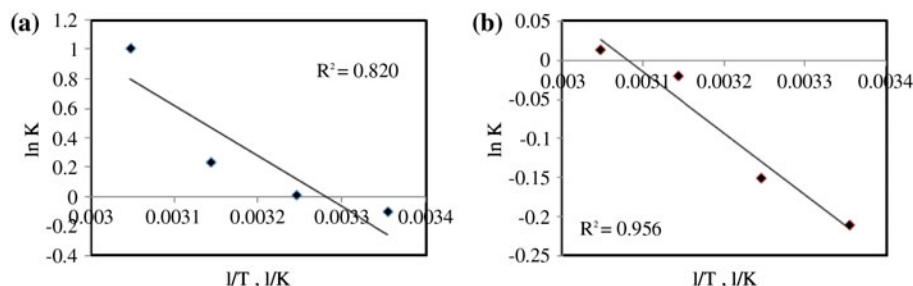


Fig. 10. The plots of  $\ln K$  vs.  $1/T$  for adsorption of CPH onto (a) AA and (b) CFA at temperatures of 298, 308, 318, and 328 K.

Table 7  
Thermodynamic parameters for adsorption of CPH

Adsorbate	Adsorbent	Temperature (K)	$\Delta G^\circ$ (kJ/mol)	$\Delta H^\circ$ (kJ/mol)	$\Delta S^\circ$ (kJ/mol K)	Refs.
Penicillin G	<i>R. arrhizus</i>	298	-3.4	37.2	0.137	[45]
	Activated sludge	298	-2.5	20.74	0.078	
	Activated carbon	298	-1.4	87.28	0.297	
Tetracycline	Silica	296	-8.35	-0.015	-0.025	[46]
		303	-8.21			
		310	-8.00			
Cefotaxime sodium	Polymercoated ion exchange resin T <sub>1</sub> microparticle	298	-11.27	0.017	0.096	[47]
		308	-12.23			
		313	-12.71			
Ciprofloxacin	CFA	298	-10.44	0.016	0.091	[23]
		308	-11.36			
		313	-11.82			
CPH	Soil	303	-2.82	14.88	0.058	[23]
		313	-2.89		0.056	
		323	-2.97		0.055	
CPH	CFA	288	-14.10	38.53	0.306	[48]
		308	-2.72	85.47	0.1426	
		308	0.399	6.572	0.020	
CPH	AA	318	0.044			Present study
		328	-0.029			
		298	0.248	28.408	0.093	
		308	-0.030			
		318	-0.620			
		328	-2.714			

47.76%. Similar results indicating an increase in removal with increase in initial CPH concentration were also reported by Zhang et al. [23] when modified CFA was used as an adsorbent.

### 3.7. Thermodynamic studies

In reference to the kinetic studies, removal of CPH is enhanced at higher temperature indicating the endothermic nature of adsorption. The prediction was further confirmed by the calculation of enthalpy change ( $\Delta H^\circ$ ) using Van't Hoff equation. Curves were plotted with  $\ln K$  as ordinate and  $1/T$  as abscissa for adsorption of CPH on CFA and AA and are shown in Fig. 10(a) and (b).

The corresponding values of enthalpy, entropy, and free energy estimated from Fig. 10(a) and (b) have been reported in Table 7. From adsorption studies of CPH using CFA and AA, it is evident that value of Gibb's free energy is positive at lower temperatures while it is negative at high temperatures, while the entropy and enthalpy are positive. This suggests that the process is spontaneous at high temperatures and exhibits endothermicity. The process was more spontaneous in case of AA as compared to CFA. Overall, it can be stated that for adsorption of CPH to be spontaneous, the temperature of the system should be kept high. Thermodynamic data from previous studies on adsorption of various antibiotics on different adsorbents have been reported in Table 7.

The spent adsorbent can be reused after proper regeneration. Various regeneration procedures such as acid/alkali regeneration, thermal regeneration, solvent extraction, etc. have been adopted by researchers depending upon the type of adsorbate-adsorbent system [49]. In the present study, AA may be regenerated by caustic regeneration while regeneration of CFA may be achieved by  $H_2O_2$  treatment [50], alkali regeneration [11], or thermal regeneration procedure.

## 4. Conclusions

The adsorption of CPH on AA and CFA as a function of the adsorbate concentration, adsorbent dose, pH, and temperature was investigated. AA as an adsorbent performed better in comparison to CFA for the removal of CPH. Maximum removal of 98% was obtained with an optimal dose of 5 g/L of AA at the natural pH of aqueous solution. Equilibrium was achieved practically in 300 min for AA and 270 min for CFA. Adsorption followed Freundlich isotherm in case of both AA and CFA. From the isotherm analysis, it was found that for CFA, chemisorption was dominant. However, for AA, cooperative adsorption was the leading phenomenon.

Adsorption kinetics and error analysis in both cases of adsorbents confirmed the applicability of pseudo-second-order kinetic model. It was found that intraparticle diffusion was not the only factor that controlled the adsorption process. Elovich kinetic constants indicated that initial adsorption rate ( $\alpha$ ) for AA and CFA was always greater than desorption rate. Considering  $q_{e,exp}$  values over a range of initial CPH concentrations and temperatures, AA and CFA both perform better at higher concentration (90 mg/L) and at higher temperature (55°C).

The effect of various parameters such as adsorbent dose, adsorbate concentration, pH, and temperature on removal of CPH by AA and CFA was also examined. Significant removal of CPH was found under acidic conditions with optimal removal at pH 4. At pH 4, higher removal (76.67%) of CPH was obtained with AA in contrast to the removal (48.89%) obtained with CFA. Higher the concentration of adsorbate, higher was the removal and vice versa. Moreover, the adsorption of CPH was found to increase with an increase in temperature indicating the endothermic nature which was later confirmed by thermodynamic studies also. The process was more feasible and spontaneous for AA as compared to CFA.

Overall, it can be concluded that AA is a better adsorbent than CFA for the removal of CPH from its aqueous solution. The results obtained in the study can further be utilized in designing the wastewater treatment plants for the removal of CPH.

## Acknowledgments

One of the authors, Ms Monika Maheshwari is thankful to The Council of Scientific and Industrial Research (CSIR), New Delhi, India for the award of SRF.

## Nomenclature

$q_e$	—	adsorption capacity at equilibrium (mg/g)
$q_t$	—	adsorption capacity at time $t$ (mg/g)
$k_1$	—	pseudo-first-order rate constant of adsorption ( $\text{min}^{-1}$ )
$k_2$	—	pseudo-second-order rate constant of adsorption (g/mg min)
$C^*$	—	thickness of boundary layer
$K_{dif}$	—	intraparticle diffusion rate constant ( $\text{mg/g min}^{0.5}$ )
$q_{e,calc}$	—	adsorption capacity at equilibrium calculated for kinetics (mg/g)
$q_m$	—	max. sorption capacity (mg/g), adsorption capacity at equilibrium determined by experiments

$C_e$	— equilibrium concentration of the adsorbate (mg/L)
$K_L$	— Langmuir constants (L/mg)
$C_0$	— initial concentration of antibiotic (mg/L)
$b_T$	— Temkin constant related to the heat of adsorption (J/mol)
$a_T$	— equilibrium binding constant corresponding to the maximum binding energy (L/mg)
$\Delta G^\circ$	— Gibb's free energy (kJ/mol)
$\Delta H^\circ$	— enthalpy change (kJ/mol)
$\Delta S^\circ$	— entropy change (kJ/molK)
$\Delta R_L$	— separation factor
$T$	— temperature in K
$E_a$	— Arrhenius activation energy (kJ/mol)
$A$	— Arrhenius factor
$R$	— universal gas constant
$\alpha$	— initial adsorption rate (mg/g min)
$\beta$	— desorption constant (g/mg)

## References

- [1] K.J. Choi, S.G. Kim, S.H. Kim, Removal of antibiotics by coagulation and granular activated carbon filtration, *J. Hazard Mater.* 151 (2008) 38–43.
- [2] K. Fent, A.A. Weston, D. Caminada, Ecotoxicology of human pharmaceuticals, *Aquat. Toxicol.* 76 (2006) 122–159.
- [3] C. Carlesi Jara, D. Fino, V. Specchia, G. Saracco, P. Spinelli, Electrochemical removal of antibiotics from wastewaters, *Appl. Catal. B-Environ.* 70 (2007) 479–487.
- [4] M. Berlanga, M.T. Montero, J. Hernandez-Borrell, M. Vinas, Influence of the cell wall on ciprofloxacin susceptibility in selected wild-type Gram-negative and Gram-positive bacteria, *Int. J. Antimicrob. Ag.* 23 (2004) 627–630.
- [5] A. Bhandari, L.I. Close, W. Kim, R.P. Hunter, D.E. Koch, R.Y. Surampalli, Occurrence of ciprofloxacin, sulfamethoxazole, and azithromycin in municipal wastewater treatment plants, *Pract. Period. Hazard. Toxic Radioact. Waste Manage.* 12 (2008) 275–281.
- [6] R. Chouhan, A.K. Bajpai, Release dynamics of ciprofloxacin from swellable nanocarriers of poly (2-hydroxyethyl methacrylate): An in vitro study, *Nanomed. Nanotech. Biol. Med.* 6 (2010) 453–462.
- [7] K. Kummerer, Significance of antibiotics in the environment, *J. Antimicrob. Chemoth.* 52 (2003) 5–7.
- [8] K.D. Brown, J. Kulis, B. Thomson, T.H. Chapman, D.B. Mawhinney, Occurrence of antibiotics in hospital, residential, and dairy effluent, municipal wastewater, and the Rio Grande in New Mexico, *Sci. Total Environ.* 366 (2006) 772–783.
- [9] D.T. Sponza, P. Demirden, Treatability of sulfamerazine in sequential upflow anaerobic sludge blanket reactor (UASB)/completely stirred tank reactor (CSTR) processes, *Sep. Purif. Technol.* 56 (2007) 108–117.
- [10] C.J. Eboka, A.B. Afolabi, In-vitro adsorption of fluoroquinolones on some pharmaceutical adsorbents, *Trop. J. Pharm. Res.* 5 (2007) 533–538.
- [11] H. Zhang, C.H. Huang, Adsorption and oxidation of fluoroquinolone antibacterial agents and structurally related amines with goethite, *Chemosphere* 66 (2007) 1502–1512.
- [12] S.P. Sun, H.Q. Guo, Q. Ke, J.H. Sun, S.H. Shi, M.L. Zhang, Q. Zhou, Degradation of antibiotic ciprofloxacin hydrochloride by photo-Fenton oxidation process, *Environ. Eng. Sci.* 26 (2009) 753–759.
- [13] E.S. Elmolla, M. Chaudhuri, Photocatalytic degradation of amoxicillin, ampicillin and cloxacillin antibiotics in aqueous solution using UV/TiO<sub>2</sub> and UV/H<sub>2</sub>O<sub>2</sub>/TiO<sub>2</sub> photocatalysis, *Desalination* 252 (2010) 46–52.
- [14] B. De Witte, J. Dewulf, K. Demeestere, H. Van Langenhove, Ozonation and advanced oxidation by the peroxone process of ciprofloxacin in water, *J. Hazard. Mater.* 161 (2009) 701–708.
- [15] M. Deborde, U. Von Gunten, Reactions of chlorine with inorganic and organic compounds during water treatment – kinetics and mechanisms: A critical review, *Water Res.* 42 (2008) 13–51.
- [16] M.R. Senapati, Fly ash from thermal power plants – waste management and overview, *Curr. Sci. India* 100 (2011) 1791–1794.
- [17] W. Bouguerra, M. Ben Sik Ali, B. Hamrouni, M. Dhahbi, Equilibrium and kinetic studies of adsorption of silica onto activated alumina, *Desalination*, 206 (2007) 141–146.
- [18] T. Su, X. Guan, G. Gu, J. Wang, Adsorption characteristics of As (V), Se (IV), and V (V) onto activated alumina: Effects of pH, surface loading, and ionic strength, *J. Colloid Interf. Sci* 326 (2008) 347–353.
- [19] S.P. Kamble, G. Deshpande, P.P. Barve, S. Rayalu, N.K. Labhsetwar, A. Malyshev, B.D. Kulkarni, Adsorption of fluoride from aqueous solution by alumina of alkoxide nature: Batch and continuous operation, *Desalination* 264 (2010) 15–23.
- [20] C.J. Wang, Z. Li, W.T. Jiang, J.S. Jean, C.C. Liu, Cation exchange interaction between antibiotic ciprofloxacin and montmorillonite, *J. Hazard. Mater.* 183 (2010) 309–314.
- [21] P. Punyapalikul, T. Sitthisorn, Removal of ciprofloxacin and carbamazepine by adsorption on functionalized mesoporous silicates, *World Acad. Sci. Eng. Tech.* 69 (2010) 546–550.
- [22] S.A.C. Carabineiro, T. Thavorn-amornsri, M.F.R. Pereira, P. Serp, J.L. Figueiredo, Comparison between activated carbon, carbon xerogel and carbon nanotubes for the adsorption of the antibiotic ciprofloxacin, *Catal. Today* 186 (2012) 29–34.
- [23] C.L. Zhang, G.L. Qiao, F. Zhao, Y. Wang, Thermodynamic and kinetic parameters of ciprofloxacin adsorption onto modified coal fly ash from aqueous solution, *J. Mol. Liq.* 163 (2011) 53–56.
- [24] Z. Li, H. Hong, L. Liao, C.J. Ackley, L.A. Schulz, R.A. MacDonald, A.L. Mihelich, S.M. Emard, A mechanistic study of ciprofloxacin removal by kaolinite, *Colloid Surf. B* 88 (2011) 339–344.
- [25] D. Vasudevan, G.L. Bruland, B.S. Torrance, V.G. Upchurch, A.A. MacKay, PH-dependent ciprofloxacin sorption to soils: Interaction mechanisms and soil factors influencing sorption, *Geoderma* 151 (2009) 68–76.
- [26] D.G. Larsson, C. De Pedro, N. Paxeus, Effluent from drug manufactures contains extremely high levels of pharmaceuticals, *J. Hazard. Mater.* 148 (2007) 751–755.
- [27] L. Fratini, E.E.S. Schapoval, Ciprofloxacin determination by visible light spectrophotometry using iron (III) nitrate, *Int. J. Pharm.* 127 (1996) 279–282.
- [28] K.G. Bhattacharyya, A. Sharma, Kinetics and thermodynamics of Methylene Blue adsorption on Neem (*Azadirachta indica*) leaf powder, *Dyes Pig.* 65 (2005) 51–59.
- [29] M.K. Purkait, A. Maiti, S. DasGupta, S. De, Removal of congo red using activated carbon and its regeneration, *J. Hazard. Mater.* 145 (2007) 287–295.
- [30] M. Dogan, Y. Ozdemir, M. Alkan, Adsorption kinetics and mechanism of cationic methyl violet and methylene blue dyes onto sepiolite, *Dyes Pig.* 75 (2007) 701–713.
- [31] A.E. Nemr, Potential of pomegranate husk carbon for Cr (VI) removal from wastewater: Kinetic and isotherm studies, *J. Hazard. Mater.* 161 (2009) 132–141.
- [32] A.A. Augustine, B.D. Orike, A.D. Edidiong, Adsorption kinetics and modeling of Cu (II) ion sorption from aqueous solution by mercaptoacetic acid modified cassava (manihot sculenta cranz) wastes, *EJEAFChe* 6 (2007) 2221–2234.

- [33] S.M. Mak, B.T. Tey, K.Y. Cheah, W.L. Siew, K.K. Tan, Porosity characteristics and pore developments of various particle sizes palm kernel shells activated carbon (PKSAC) and its potential applications, *Adsorption* 15 (2009) 507–519.
- [34] N. Barka, A. Assabbane, A. Nounah, L. Laanab, Y.A. Ichou, Removal of textile dyes from aqueous solutions by natural phosphate as a new adsorbent, *Desalination* 235 (2009) 264–275.
- [35] E. Demirbas, M.Z. Nas, Batch kinetic and equilibrium studies of adsorption of Reactive Blue 21 by fly ash and sepiolite, *Desalination* 243 (2009) 8–21.
- [36] K.Y. Foo, B.H. Hameed, Insights into the modeling of adsorption isotherm systems, *Chem. Eng. J.* 156 (2010) 2–10.
- [37] S.A. Dastgheib, D.A. Rockstraw, A systematic study and proposed model of the adsorption of binary metal ion solutes in aqueous solution onto activated carbon produced from pecan shells, *Carbon* 40 (2002) 1853–1861.
- [38] Y.S. Ho, G. McKay, Pseudo-second order model for sorption processes, *Process Biochem.* 34 (1999) 451–465.
- [39] J. Kiurski, S. Adamovic, I. Oros, J. Krstic, I. Kovacevic, Adsorption feasibility in the Cr (total) ions removal from waste printing developer, *Global NEST J.* 14 (2012) 18–23.
- [40] J.C. Igwe, A.A. Abia, Equilibrium sorption isotherm studies of Cd (II), Pb (II) and Zn (II) ions detoxification from waste water using unmodified and EDTA-modified maize husk, *Electron. J. Biotech.* 10 (2007) 536–548.
- [41] B. Ucar, A. Guvenc, U. Mehmetoglu, Use of aluminium hydroxide sludge as adsorbents for the removal of reactive dyes: Equilibrium, thermodynamic, and kinetic studies, *Hydrol. Current. Res.* 2 (2011) 2.
- [42] B.A. Shah, A.V. Shah, P.M. Shah, Sorption isotherms and column separation of Cu (II) and Zn (II) using ortho substituted benzoic acid chelating resins, *Arch. Appl. Sci. Res.* 3 (2011) 327–341.
- [43] K. Kummerer, *Pharmaceuticals in the Environment: Sources, Fate, Effects and Risks*, Springer Verlag, 2004.
- [44] D. Mohan, K.P. Singh, G. Singh, K. Kumar, Removal of dyes from wastewater using flyash, a low-cost adsorbent, *Ind. Eng. Chem. Res.* 41 (2002) 3688–3695.
- [45] Z. Aksu, O. Tunc, Application of biosorption for penicillin G removal: Comparison with activated carbon, *Process Biochem.* 40 (2005) 831–847.
- [46] I. Turku, T. Sainio, E. Paatero, Thermodynamics of tetracycline adsorption on silica, *Environ. Chem. Lett.* 5 (2007) 225–228.
- [47] S. Vasiliu, I. Bunia, S. Racovita, V. Neagu, Adsorption of cefotaxime sodium salt on polymer coated ion exchange resin microparticles: Kinetics, equilibrium and thermodynamic studies, *Carbohydr. Polym.* 85 (2011) 376–387.
- [48] K.M. Shareef, H.O. Ahmed, Thermodynamics of equilibrium adsorption of antibiotics at solid–liquid interface, in: *Proceed. 2nd Int. Conf. Maritime Naval Sci. Eng. (MN '09) Transilvania Univ. Brasov, Romania, 2009*, pp. 129–139.
- [49] M. Sharma, R.K. Vyas, K. Singh, A review on reactive adsorption for potential environmental applications, *Adsorption* 19 (2013) 161–188.
- [50] M. Ahmaruzzaman, A review on the utilization of fly ash, *Prog. Energ. Combust.* 36 (2010) 327–363.